

## HABIT AND COMPOSITION OF GOLD GRAINS IN QUARTZ VEINS FROM GREENSTONE BELTS: IMPLICATIONS FOR MECHANISMS OF PRECIPITATION OF GOLD

DOMINIQUE MICHEL

*Ecole Nationale Supérieure de Géologie, BP 452, 54000 Nancy Cedex, France*

GASTON GIULIANI

*Institut Français de Recherche Scientifique pour le Développement en Coopération, TOA, UR13,  
213, rue La Fayette, 75480 Paris Cedex 10 et Centre de Recherches Pétrographiques et Géochimiques,  
BP 20, 54500 Vandoeuvre-lès-Nancy Cedex, France*

### ABSTRACT

The gold deposits of Fazenda Brasileiro (Bahia State) and Maria Lázara (Goiás State) in Brazil, and of Sigma at Val d'Or (Quebec) are mesothermal gold-quartz veins in greenstones terranes. The textural sites of gold grains, combined with variations in their Au:Ag ratio, show that most of the gold is secondary. Successive episodes of gold deposition in each textural site are linked to repeated deformation related to vein formation. The habit of gold grains shows the importance of surfaces of sulfides and Fe-rich minerals (tourmaline, biotite) for gold deposition. Gold reduction on earlier-formed minerals seems to be the main process of gold deposition in the three deposits studied.

*Keywords:* gold, quartz veins, textural sites, Ag contents, gold habits, precipitation.

### SOMMAIRE

Les gisements d'or de Fazenda Brasileiro et de Maria Lázara (Brésil) et de Sigma (Québec) sont des gisements mésothermaux de type veine de quartz associés à des ceintures de roches vertes. L'étude comparative entre les différents sites texturaux des grains d'or et leurs teneurs en argent respective montre que la précipitation de l'or est secondaire. Les phases successives de dépôt de l'or dans chaque site textural sont à relier à de multiples épisodes de déformation liés à la formation des veines de quartz. L'étude de la morphoscopie des grains d'or révèle l'importance de la surface des sulfures et des minéraux riches en fer (tourmaline, biotite) pour la précipitation de l'or. La réduction de l'or à la surface de minéraux préexistants semble être un processus majeur de précipitation de l'or dans les trois gisements étudiés.

*Mots-clés:* or, veines de quartz, sites texturaux, teneurs en Ag, morphoscopie, précipitation.

### INTRODUCTION

Mesothermal gold-bearing quartz veins from greenstones terranes show signs of a complex history. In most veins, features of both growth and deformation are observed. Most authors have interpreted features of deformation to be superimposed on already developed veins, with gold occupying late structural sites within the veins (Robert & Kelly 1987, Cathelineau *et al.* 1991). However, recent studies have revealed that the formation of veins results from a complex sequence of stages of growth and deformation related to repeated cycles of opening and collapse (Boullier & Robert 1992, Robert *et al.* 1995). In such deposits, grains of

gold occupy both secondary sites within the veins (fractures, boundaries along recrystallized grains) and primary sites within quartz or sulfides (euhedral or anhedral inclusions). Secondary sites are the more common.

The Ag content of gold grains varies between 25 and 10% (atomic proportion) and, most commonly, lies in the range from 13 to 15 at.% (Boyle 1979). There have been few systematic investigations on how the Ag contents of grains of gold vary with respect to their textural sites. Such investigations may provide key information on the history of gold precipitation within the deposits, *i.e.*, in a single stage or in multiple stages.

The processes of precipitation of gold suggested by

most investigators are conductive cooling, phase separation or boiling, mixing of solutions and fluid-rock reactions (Seward 1989, Shenberger & Barnes 1989). In the latter case, gold deposition was related to sulfidation reactions in the wallrock (Phillips & Groves 1984) or to a later adsorption of aqueous gold species onto earlier-formed sulfides (Starling *et al.* 1989).

Many experimental studies have shown that the various mechanisms of precipitation of gold are reflected in the textures of the precipitated gold (Machairas 1970, Jean & Bancroft 1985). Therefore, it should be possible to infer some of the processes responsible for the precipitation of gold from studies of textural habits of gold grains. We report here on textural sites of gold grains and possible related variations in Au:Ag ratio, and on habits of gold grains in selected samples from the Brazilian deposits

Fazenda Brasileiro (Bahia State) and Maria Lázara (Goiás State), and from the Sigma deposit (Val d'Or, Quebec).

#### GEOLOGY OF THE DEPOSITS

The Fazenda Brasileiro mine is located in the southern part of the Lower Proterozoic Rio Itapicuru greenstone belt, on the eastern margin of the São Francisco Craton (Fig. 1). The gold deposits lie within a mafic sill that extends east-west for 8 km, at the contact between tholeiitic basalts and a sequence of pelitic schist and psammite, approximately 1 km north of the granodiorite dome of Barrocas. The lithological contacts and the main tectonic foliation are subparallel and dip between 40° and 70° south (Reinhardt & Davison 1990, Teixeira *et al.* 1990). The gold ore is mainly located in chlorite-magnetite schist derived

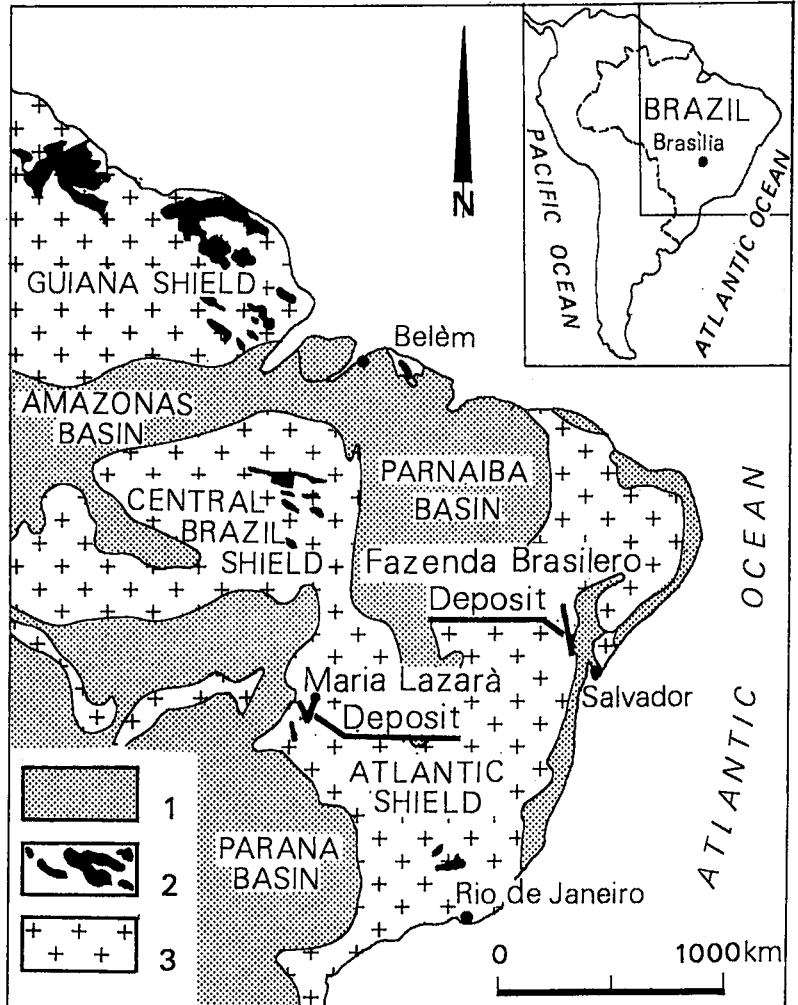


FIG. 1. Location map of the Fazenda Brasileiro (Bahia) and Maria Lázara (Goiás) deposits in Brazil. Patterns: 1 Phanerozoic formations, 2 greenstones belts, 3 Precambrian terranes.

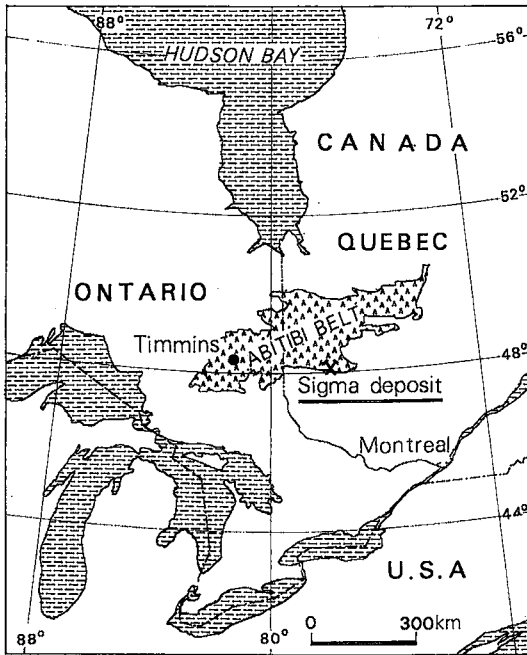


FIG. 2. Location map of the Sigma deposit (Val d'Or) in Canada.

from the mafic sill and consists of veins and veinlets enveloped by a zone of hydrothermal alteration (carbonatization, albitization, sulfidation).

The mineralized veins postdate ductile *D1* shearing and are related to steeply dipping ductile–brittle shears and associated folding of a major *D2* event during north–south shortening (Teixeira *et al.* 1990, Reinhardt & Davison 1990). They occur as thin veins concordant with *S1*, but primarily as veins discordant with *S1*, sigmoidal *en échelon* veins, tabular weakly deformed veins with incipient boudinage, and as irregular lenticular masses in *F2* fold hinges, having subvertical discordant contacts with *S1* (Reinhardt & Davison 1990). The highest-grade zones, called “breccia”, correspond to zones of abundant veins, where the intense metasomatism of the wallrock produced a bleached quartz – carbonate – albite – arsenopyrite – pyrite assemblage in which the outline of individual veins is difficult to recognize.

The Maria Lázara mine is located in the Archean Guarinos greenstone belt, in the eastern portion of the Goiás Massif, central Brazil (Fig. 1). It occurs at the contact between Archean metabasalt and tonalitic gneiss in a NW–SE-trending shear zone, at a triple-point structure, in the southern portion of a synkinematic trondhjemitic intrusive body (Pulz *et al.* 1991). An episode of ductile deformation transformed the supracrustal rocks into mylonite and ultramylonite

(Pulz 1990). The gold–quartz veins and veinlets occur in a halo of hydrothermal alteration (propylitization, biotitization ± K-feldspathization, sulfidation) that overprints the ultramylonite. The veins are synchronous with shear-zone deformation and appear as a “chocolate slab” within the mylonitic foliation (Pulz *et al.* 1991).

The Sigma deposit is located in the Val d'Or district of Quebec, in the southeastern part of the Archean Abitibi greenstone belt of the Superior Province (Fig. 2). It is hosted by metavolcanic rocks intruded by pre-ore diorite plutons. Gold occurs in steeply dipping veins in shear zones, and in subhorizontal extensional veins in extensional fractures, enveloped by a halo of hydrothermal alteration (carbonatization, sericitization, sulfidation), which developed during the last stages of *D2* N–S compression (Robert & Brown 1986). Most of the subhorizontal extensional veins occur in diorite intrusions and consist of quartz and tourmaline with minor amounts of carbonates, scheelite, pyrite and gold. The tourmaline belongs to the schorl–dravite series, with a MgO/FeO ratio close to 1 (Robert & Brown 1986).

The present study focusses on samples from the “breccia” zones of the C body at Fazenda Brasileiro, the shear-related veins of the potassic alteration zone at Maria Lázara, and a subhorizontal extensional vein at Sigma.

#### PARAGENETIC RELATIONS OF GOLD TO OTHER MINERALS

##### *Fazenda Brasileiro*

The abundant veins of the “breccia” zones led to intense alteration of the wallrock. The sequence of deposition of the main vein-forming minerals, on the basis of textural relationships, clearly shows filling and post-filling events (Table 1). Descriptions of individual quartz – albite – sulfide veins and adjacent zones of hydrothermal alteration in the chlorite–magnetite schist are given in Marimon *et al.* (1986).

TABLE 1. PARAGENETIC DIAGRAM FOR THE MAIN VEIN MINERALS OF THE FAZENDA BRASILEIRO DEPOSIT

	Filling	Post-filling
Albite ± Oligoclase	—	—
Carbonates	—	—
Quartz	—	—
Chlorite	—	—
S-rich arsenopyrite	—	—
Pyrite	—	—
Pyrrhotite	—	—
Chalcopyrite	—	—
Gold	—	—

Dotted lines represent uncertainties. See text for explanations.

TABLE 2. PARAGENETIC DIAGRAM FOR THE MAIN VEIN MINERALS OF THE MARIA LAZARA DEPOSIT

	Filling	Post-filling
Garnet	—	
Biotite	—	—
Plagioclase		—
Carbonates	—	—
Chlorite		—
Quartz	— — — —	— — — —
S-rich arsenopyrite	—	
As-rich arsenopyrite		— — — —
Gold		—
Au-Bi-Te-S grains	— — — —	— — — —

Dotted lines represent uncertainties. See text for explanations.

In the filling event, albite and, to a lesser extent, oligoclase crystals coat the vein walls, to which they are subperpendicular, and are associated with a first generation of carbonates (calcite and ankerite). At this stage, porphyroblasts of S-rich arsenopyrite (60% of total sulfides) develop at the vein walls and adjacent wallrocks (Table 2). Ilmenite inclusions in arsenopyrite are ubiquitous and show a common orientation. The central part of the veinlets is filled by large grains of quartz showing undulose extinction. In some cases, small grains of quartz occur along the boundaries of the large grains.

The post-filling event produced fracturing of all above-mentioned main vein-forming minerals, with subsequent precipitation of carbonates, quartz, pyrite (or pyrrhotite) and, to a lesser extent, chlorite and chalcopyrite (Table 1).

A second generation of calcite occurs along fractures (Fig. 3A) or in pressure shadows of porphyroblasts of arsenopyrite (Fig. 3B). Along fractures, calcite crystals are perpendicular to the edges of arsenopyrite (Fig. 3C) and are variably associated with pyrite or chalcopyrite. The fracturing of arsenopyrite may be intense, with fragments included in calcite. In pressure shadows, calcite grains occur with quartz and are rarely replaced by chlorite and pyrite.

Pyrite clearly postdates arsenopyrite, as cross-cutting veinlets (Fig. 3D) or as overgrowths. It is associated with variable amounts of chalcopyrite and carbonates. Pyrite also occurs as grains impregnating either albite (Fig. 3E) at the vein wall, or filling cavities in quartz aggregates in the central part of the veins (Fig. 3F). In the latter case, pyrite and then carbonates precipitated between aggregates of quartz. In deeper samples, pyrite is replaced by pyrrhotite. The pyrite does not contain Co, Ni or As.

#### Gold at Fazenda Brasileiro

Almost all grains of gold are closely spatially related

to S-rich arsenopyrite. In a first textural site, they occur along fractures in contact with arsenopyrite, with or without variable amounts of calcite (Fig. 4C), pyrite (Fig. 3D) and, rarely, chalcopyrite. Within a single grain of arsenopyrite, gold lies along distinct fractures that are variously oriented (Figs. 4A, B). The gold obviously occupies secondary sites linked to post-filling fractures.

In a second textural occurrence, grains of gold cling to the edge of arsenopyrite grains in what may be secondary or primary sites. Some of these gold grains appear as a "bridge" between two arsenopyrite grains having a common orientation (Fig. 4D).

In a third textural occurrence, they appear as inclusions within arsenopyrite (Fig. 4E) that may be either primary sites (filling event) or secondary sites (post-filling event) because of the possible presence of concealed microfractures.

In a fourth, uncommon textural site, gold grains occur in the gangue. They appear in interstices of aggregates of quartz and carbonates close to arsenopyrite (Fig. 4F). In one case, grains of gold are located between grains of carbonate in a pressure shadow of arsenopyrite (Fig. 3B). All these sites are secondary.

#### Maria Lázara

In the wallrock-alteration zone, at the contacts of the veins, tourmaline and fine-grained sericite occur parallel to the schistosity, whereas biotite, garnet and arsenopyrite form porphyroblasts that clearly postdate the development of the schistosity.

The main vein minerals are biotite, chlorite, carbonates, arsenopyrite and quartz. Vein textures reflect two main stages of mineral deposition (Table 2), related to growth and deformation events.

In the filling event, biotite and carbonates develop with arsenopyrite at the contact of the wallrocks. The central part of the vein is occupied by quartz, the most abundant vein mineral. The arsenopyrite grains are porous (due to dissolution), with many solid inclusions (e.g., carbonates, tourmaline, ilmenite), and are S-rich (Table 2).

The features that postdate filling occur both in the veins and in the inner hydrothermally altered zone, especially as pressure shadows on arsenopyrite and biotite porphyroblasts (Fig. 5A) and, in a few cases, as veined fractures in arsenopyrite (Fig. 5B). Pressure shadows contain chlorite, biotite, quartz, rarely carbonates and plagioclase, more rarely pyrite and chalcopyrite. Vein-filled fractures variably consist of plagioclase, carbonates, white mica and quartz.

The event that postdated filling is also characterized by the presence of As-rich arsenopyrite (Table 3), free of pores and inclusions; in most cases, it forms a rim on large grains of S-rich arsenopyrite (Fig. 5C). An inclusion of silver appears in one grain of As-rich arsenopyrite.

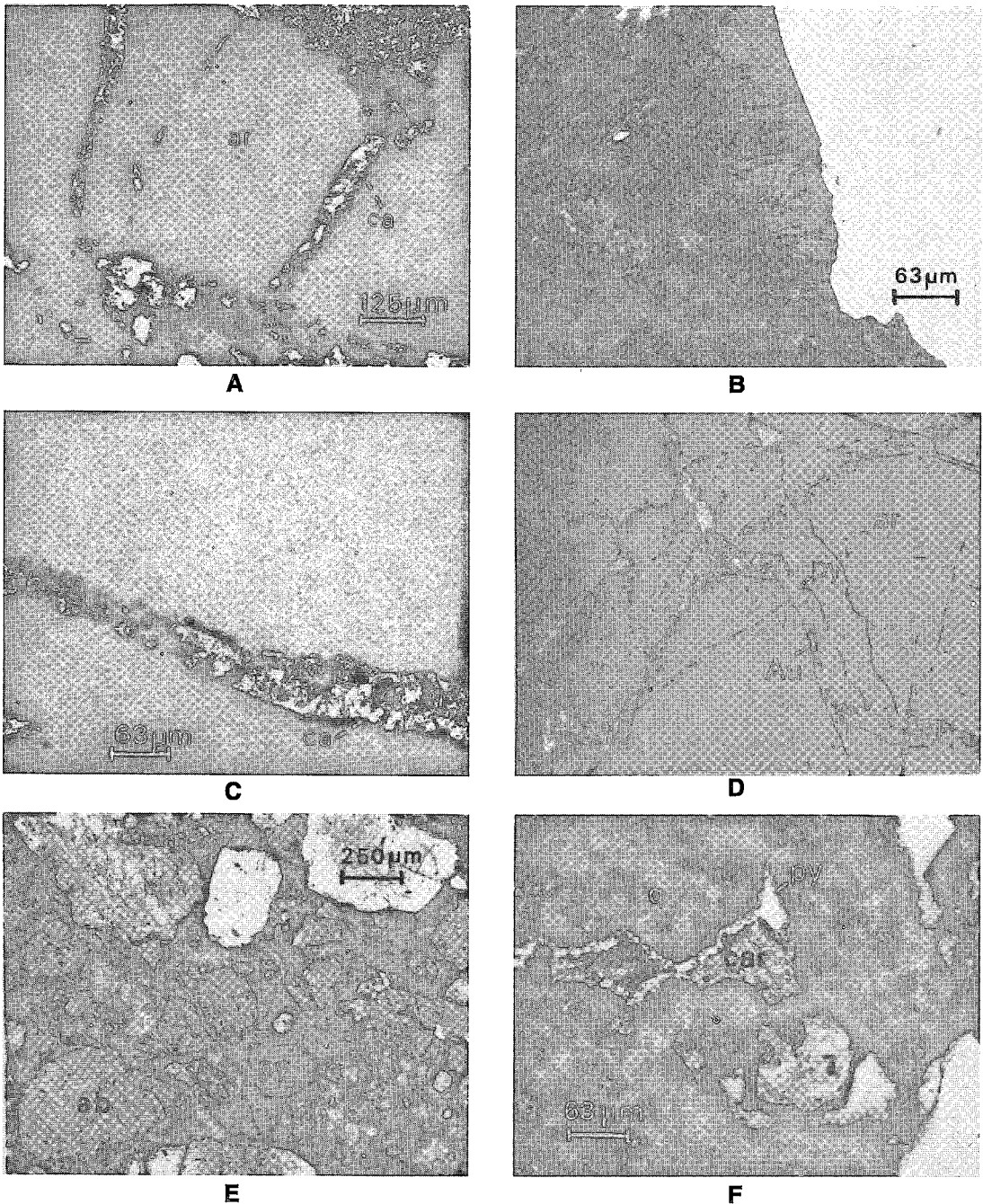
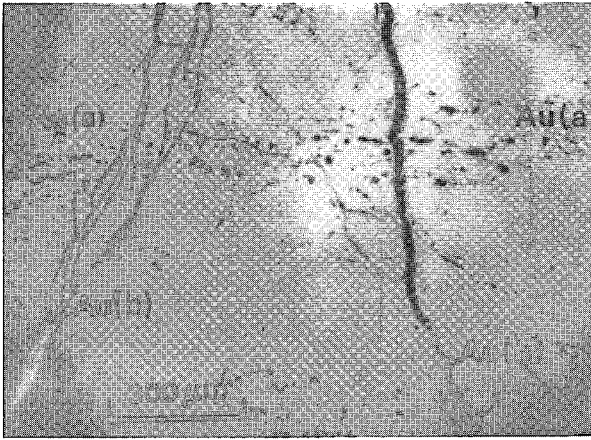
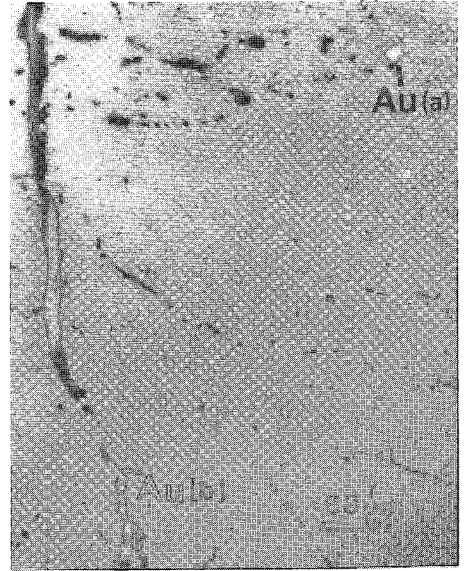


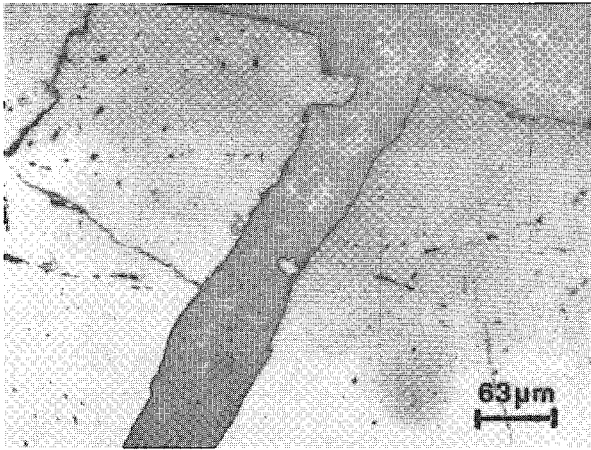
FIG. 3. Fazenda Brasileiro mine. Textural relationships among vein-forming minerals. A. Fractures in arsenopyrite (ar) veined by calcite (ca). Transmitted and reflected light, crossed polars. B. Quartz (q), calcite (ca) and gold (Au) in a pressure shadow of arsenopyrite. Transmitted and reflected plane-polarized light. C. Calcite (ca) subperpendicular to the edges of arsenopyrite. Transmitted and reflected light, crossed polars. D. Gold (Au) with pyrite (py) in arsenopyrite (ar) fractures. Reflected plane-polarized light. E. Pyrite (py) impregnating albite (ab). Transmitted and reflected plane-polarized light. F. Pyrite (py) and carbonates (car) between quartz (q) aggregates. Transmitted and reflected plane-polarized light.



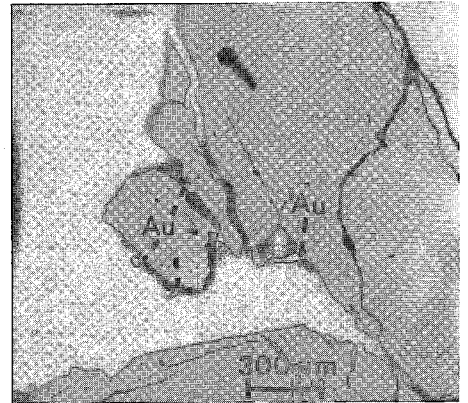
**A**



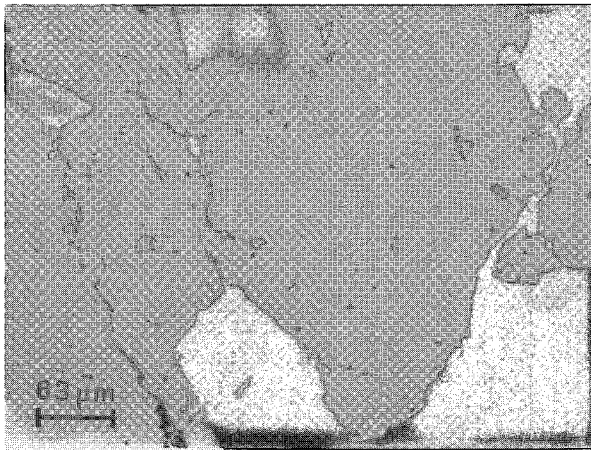
**B**



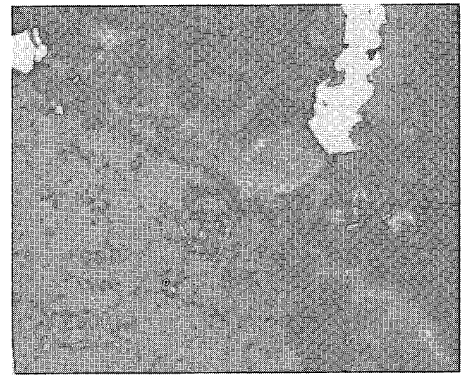
**C**



**D**



**E**



**F**



FIG. 4. Fazenda Brasileiro mine. Textural sites of gold. A. Two groups of gold grains in a S-rich arsenopyrite along differently oriented fractures. Silver contents in Au(a) and Au(b) grains are respectively 13.26 and 17.82 at.%. Reflected plane-polarized light. B. Detail on the right-hand side of A. C. Gold clung to arsenopyrite in a fracture veined by calcite. Transmitted and reflected plane-polarized light. D. Gold grains (Au) on the edge of arsenopyrite grains. Some of them look like a "bridge" between two grains of arsenopyrite having a common orientation (in crossed nicols). Reflected plane-polarized light. E. Gold inclusions (primary inclusions?) in arsenopyrite. Reflected plane-polarized light. F. Gold grains (Au) in interstices of aggregates of quartz (q) and carbonates (car). Reflected plane-polarized light.

←

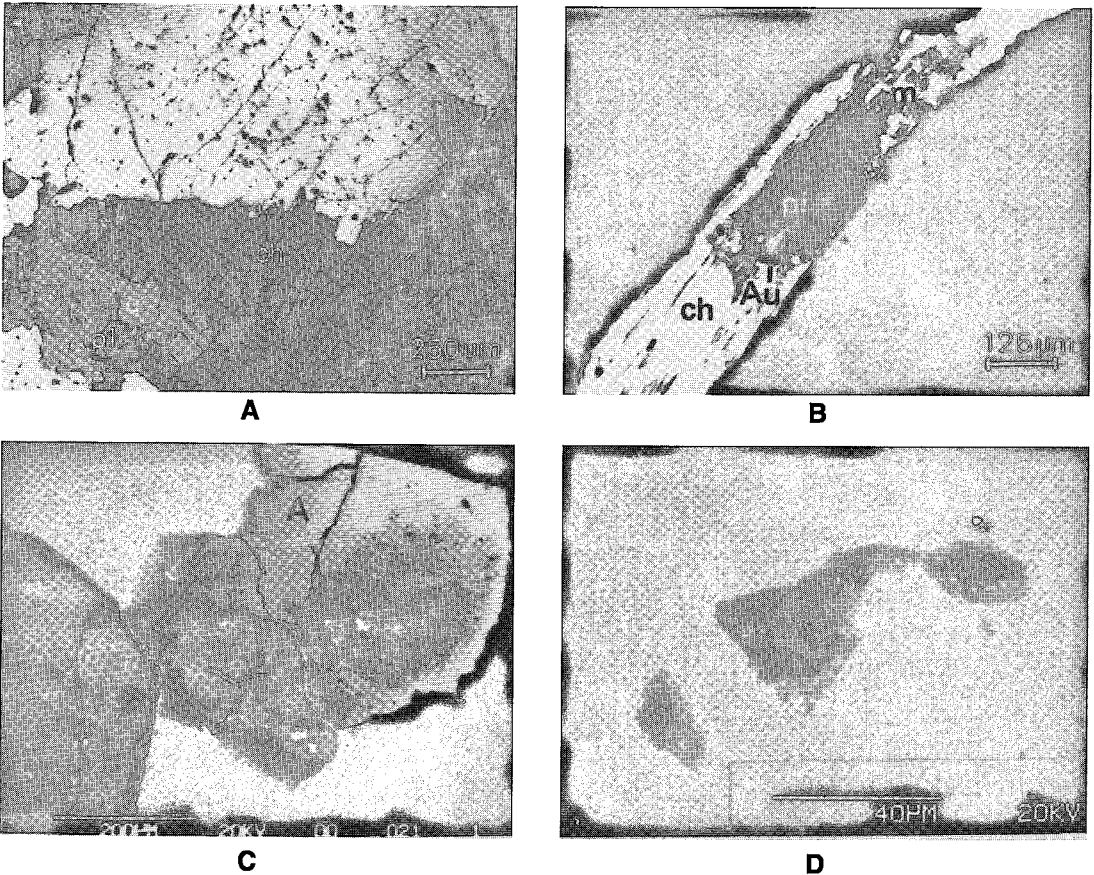


FIG. 5. Maria Lázara mine. Textural relationships among vein-forming minerals. A. Chlorite (ch), quartz (q) and plagioclase (pl) in a pressure shadow of an arsenopyrite porphyroblast. Reflected plane-polarized light. B. Veined fractures in a grain of arsenopyrite, with chlorite (ch), plagioclase (pl), muscovite (m) and gold (Au). Gold is attached to chlorite and plagioclase. Transmitted plane-polarized light. C. Zoned grain of arsenopyrite with a porous S-rich core (S) and a white As-rich rim (A). SEM photograph in the back-scattered electron mode. D. Gold (Au), joseite B ( $\text{Bi}_4\text{Te}_2\text{S}$ ; Jo) and bismuthinite ( $\text{Bi}_2\text{S}_3$ ; Bi) in an Au - Bi - Te - S multiphase grain. SEM photograph in the back-scattered electron mode.

TABLE 3. AVERAGE COMPOSITION OF ARSENOPYRITE

	Faz.Brasileiro	Mar.Lázara
As wt%	44.81	45.57
Fe wt%	34.24	33.76
S wt%	20.61	20.06
Total	99.67	99.39
As at	32.26	33.08
Fe at	33.06	32.88
S at	34.66	34.02

Average of respectively 252 and 159 quantitative electron microprobe analyses with standard sulfur deviations of 0.7 and 0.53.

### Gold at Maria Lázara

Gold occurs either as grains of gold or in multiphase aggregates of Au – Bi – Te – S minerals (Fig. 5D). The aggregates contain sheets and layered intergrowths of bismuthinite, joseite B, csiklovaite, maldonite, native gold, and only occur in samples where As-rich arsenopyrite is observed. Both types of gold grains are linked to the post-filling event and occupy secondary textural sites. In one textural occurrence, they are attached to S-rich arsenopyrite in holes that arose by dissolution (Fig. 6A), along microfractures (Fig. 6B) and at the edges of arsenopyrite grains. In another textural occurrence, they are localized in the gangue, next to arsenopyrite. They occur (i) in the innermost zone of hydrothermal alteration, between tourmaline grains (Fig. 6C), (ii) in the vein, between quartz grains (Fig. 6D). In the vein, they are also attached to partly chloritized biotite (Fig. 6E), to chlorite (Fig. 5B), or to carbonates that are alteration products of plagioclase (Fig. 6E).

### Sigma mine

Robert & Brown (1986) have shown that the extensional veins have undergone filling and post-filling events. In the filling event, the deposition of the main minerals began with calcium-bearing minerals, then tourmaline, pyrite and quartz. The event that post-dates deposition accounts for the presence of calcite, small amounts of pyrrhotite–chalcopyrite, white mica and chlorite with gold and tellurides.

### Gold at the Sigma mine

In our study, the veins were found to contain very minor amounts of sulfides, mostly pyrite, which differs from the previously described examples of Brazilian ores. Most of grains of gold are localized in secondary textural sites, attached to tourmaline along fractures and grain boundaries, in pore space, and with calcite aggregates between quartz grains. Others occur as euhedral crystals (Fig. 6F) along microfractures parallel to trails of two-phase H<sub>2</sub>O-bearing fluid

inclusions. Some of the gold grains are wetted by an unidentified fluid phase (Robert *et al.* 1995). The timing of trapping of the solid and fluid phases is still unresolved.

### CHEMICAL COMPOSITION OF GOLD GRAINS

#### Analytical procedure

Quantitative electron-microprobe (QEM) analyses of native gold were performed on polished sections with a Cameca SX microprobe (Université de Nancy I), using an accelerating voltage of 30 kV, a beam current of 60 nA, and a counting time of 30 s. The elements Au, Ag were calibrated with native elements. Gold inclusions smaller than 2 µm were not analyzed owing to the size of the excited volume under the electron beam.

#### Fazenda Brasileiro

The silver content range of gold grains at Fazenda Brasileiro does not vary among the different textural varieties of gold (Fig. 7). In the first type of secondary textural site, the grains of gold lie along fractures of the arsenopyrite with or without pyrite. They present silver contents ranging between 11.37 and 20.47 at.% (Fig. 7A).

In the second type of occurrence, the grains of gold are localized at the edge of arsenopyrite grains (either primary or secondary sites). Silver contents vary between 10.11 and 16.67 at.% (Fig. 7B) and fall within the above interval. In the third textural occurrence, the inclusions of gold (either primary or secondary sites) have Ag contents varying between 11.38 and 19.25 at.% (Fig. 7C). This interval also overlaps that of the above intervals. In the fourth secondary textural site, similar results (10.31 – 19.52 at.%) are observed for the grains of gold in the gangue (along carbonates and quartz aggregates) (Fig. 7D). Therefore, no significant difference in Ag contents is observed either between each secondary site of gold or between the secondary sites and the possible primary sites.

For each textural variety, the range in Ag content is large and could reflect differences in local conditions during precipitation of gold. But gold particles along distinct fractures within a grain of arsenopyrite have distinct Ag contents (Figs. 4A, B): 13.26 at.% for Au(a) and 17.82 at.% for Au(b), which supports the hypothesis of successive deposition of gold related to repeated events of fracturing, in each textural site.

#### Maria Lázara

Two compositional groups of gold grains have been observed. The first group has Ag contents varying between 9 and 16 at.% and occurs in all textural sites. The second group has Ag contents invariably below



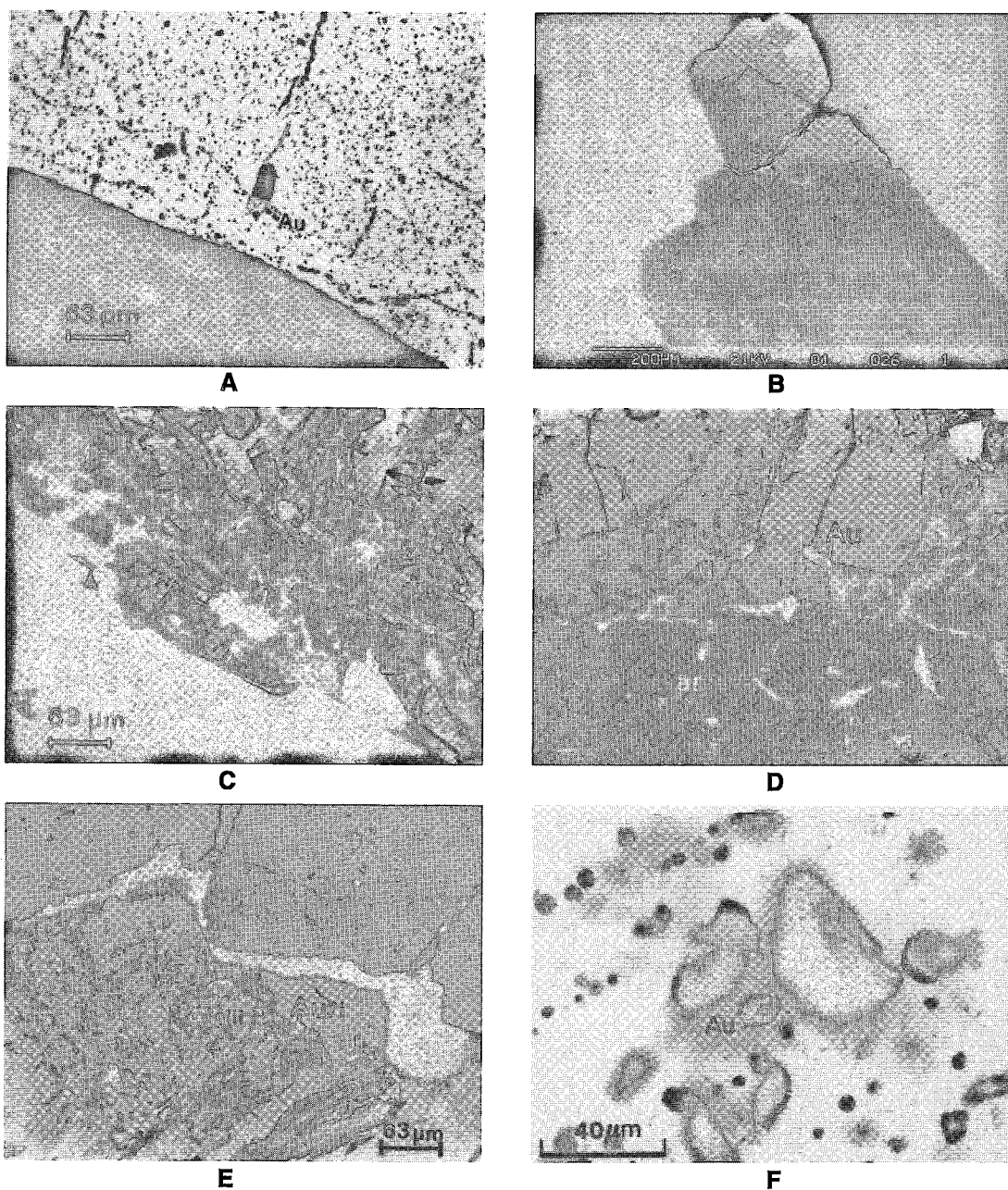


FIG. 6. María Lázara mine (A–E) and Sigma mine (F). Textural sites of gold. A. Gold (Au) inside a grain of S-rich arsenopyrite. Reflected plane-polarized light. B. Gold along a microfracture in a grain of arsenopyrite. As-rich and S-rich arsenopyrite appear, respectively, white and grey. SEM photograph in the back-scattered electron mode. C. Gold (Au) between tourmaline grains in the innermost zone of hydrothermal alteration. Transmitted light, crossed polars. D. Au – Bi – Te – S multiphase grain (Au) between quartz grains (q) beside a grain of arsenopyrite (ar). Transmitted and reflected plane-polarized light. E. Au – Bi – Te – S multiphase grains in a pressure shadow of arsenopyrite. They are attached to biotite that has undergone chloritization (Au/i) and to carbonates from a plagioclase that has undergone alteration (Au/ii). Transmitted and reflected plane-polarized light. F. Gold (Au) in fractures parallel to planes of  $H_2O \pm NaCl$  fluid inclusions in quartz (Robert *et al.* 1995).

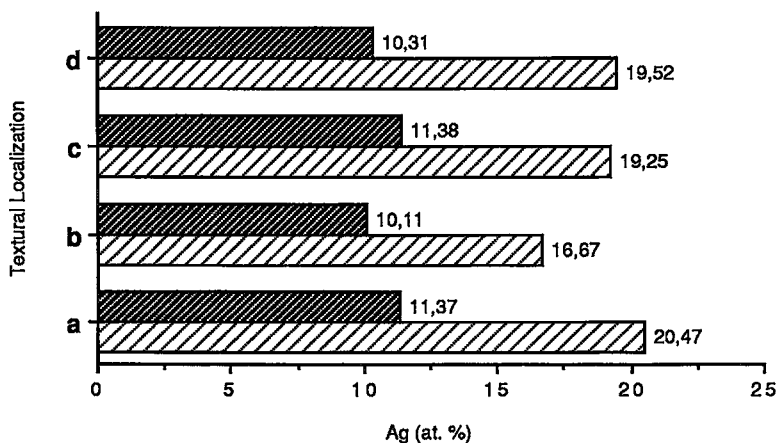


Fig. 7. Fazenda Brasileiro mine. Ranges of silver content in grains of gold in the four different textural groups (242 analyses): a) fractures of arsenopyrite with or without pyrite (113 analyses), b) edges of arsenopyrite (33 analyses), c) inclusions inside arsenopyrite (43 analyses), and d) between quartz and aggregates of carbonates close to the arsenopyrite (53 analyses).

5.5 at.% and only occurs in association with the Au – Bi – Te – S multiphase grains. Such low Ag contents were never found in the other gold grains. In a Au – Bi – Te – S multiphase grain, an external rim of this type of gold was detected around a grain of gold of the first compositional group and consequently postdates it (Michel *et al.* 1994).

The low Ag content of gold in the Bi – Te – S multiphase grains may be explained by Boyle's statement (1979): "gold appears to have a greater affinity for tellurium than for silver, and will combine with it in preference to silver", because inclusions of native silver occur in the contemporaneous As-rich arsenopyrite.

Both compositional types of gold grains occur in secondary textural sites, related to a post-filling event of deformation. The fact that the grains of Ag-poor gold postdate those of the other type reveals the presence of repeated post-filling events of gold precipitation.

#### MORPHOLOGICAL STUDY OF GOLD GRAINS

##### Analytical procedure

Gravimetric separations from sieved fractions were undertaken to concentrate sulfides and gold from the Brazilian gold-bearing samples. A cold chemical attack by concentrated HNO<sub>3</sub> dissolved the sulfides and released gold grains, which were recovered on filters under vacuum. A digestion of the quartz matrix with hydrofluoric acid was undertaken for the Sigma samples, before filtration, according to Neuberger's (1975) method. A study of the filters was carried with

a Cambridge Stereoscan 250 scanning electron microscope (Université de Nancy I) using back-scattered electron (BSE) images and energy-dispersion X-ray spectrometry (EDX) for the location of gold particles. Two hundred and ten grains were examined.

##### Crystallographic data

Gold atoms lie on the points of a face-centered cubic-closest-packing (CCP) arrangement and show a layer sequence ABCABC along a threefold axis. The forms with the highest density of atomic packing (111) are observed and correspond to octahedra. But octahedral crystals are relatively rare in natural occurrences. Growth twinning along the (111) planes accounts for the ubiquitous presence of crystals with various platy shapes in nature.

##### Fazenda Brasileiro and Maria Lázara

As a result of the analytical procedure, the gold grains recovered from the Fazenda Brasileiro and Maria Lázara ores are texturally within or close to arsenopyrite. From the paragenetic study, they correspond to the mode of occurrence of almost all the gold in both deposits.

Four morphological groups of gold grains are recognized: (1) Globular–reniform grains up to 8 µm across (Figs. 8A, B). They consist of an amalgamation of individual globules of gold that are subparallel to each other, with individual sizes ranging from 0.2 to 2 µm. These superposed and parallel planes represent (111) growth planes. They are common in both Brazilian deposits. (2) Cast-rich grains range in size

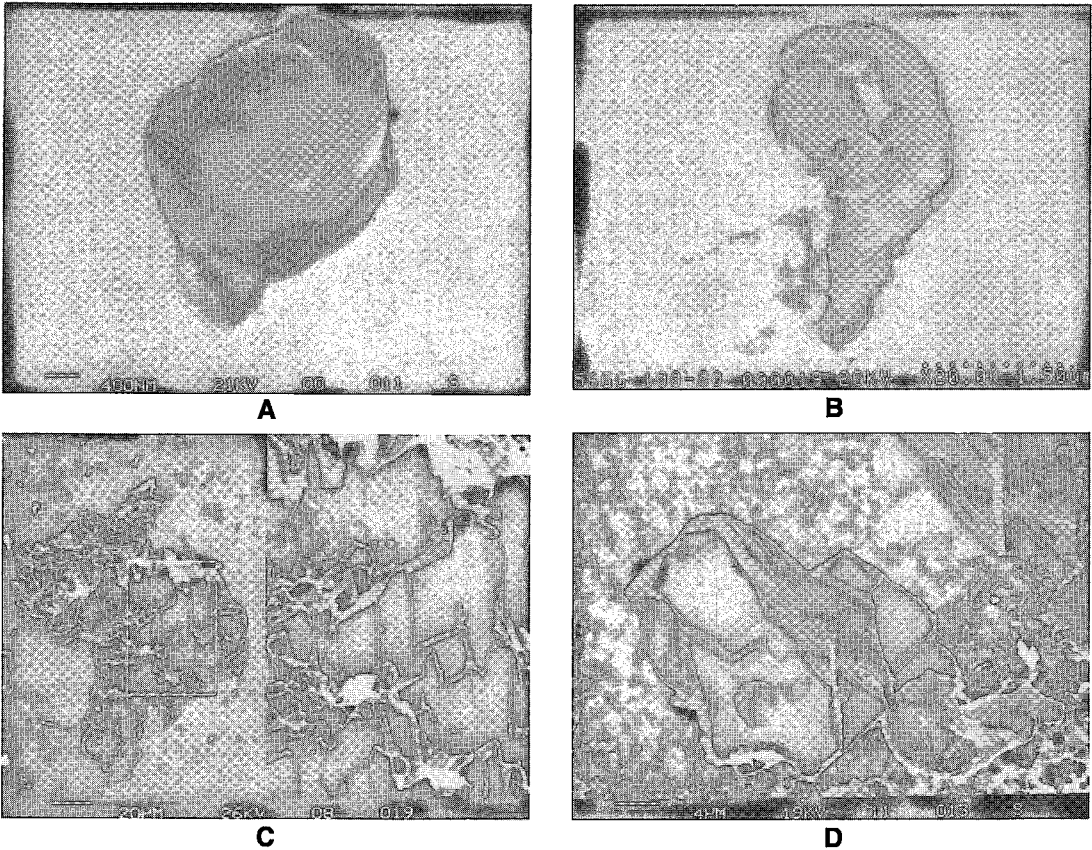


FIG. 8. The morphology of grains of gold as revealed by scanning electron microscopy. A. global-reniform grain from Fazenda Brasileiro. The grain is composed of superposed globules with sizes ranging from 0.2 to 2  $\mu\text{m}$ . B. Global-reniform grain from Maria Lázara; the stacking-up of the globules differ from A. C. Cast-rich grain from Fazenda Brasileiro, with characteristic rhombic prints indicating an arsenopyrite cast. D. Cast-rich grain from Fazenda Brasileiro with a rhombic print. On the upper right-hand side, the growth planes are parallel to the cast.

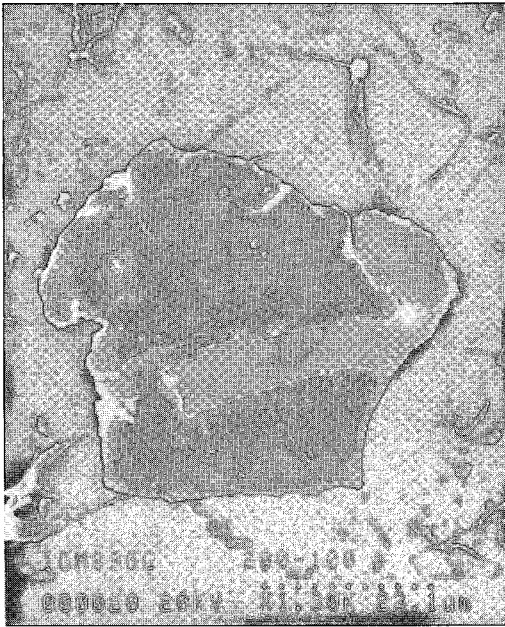
from about 10 to 100  $\mu\text{m}$  across (Figs. 8C, D). They are the most abundant, and are either irregular three-dimensional grains or plates of various thickness. Irregular or plate-shaped grains may contain casts showing host-mineral forms that are, in most instances, specific. Rhombic forms are common and characterize the imprint of arsenopyrite on gold grains. Depending on the plane of observation, growth planes parallel to the casts are visible (Fig. 8D).

Thin plates of gold are most abundant in the Maria Lázara samples (Fig. 9A). These correspond to gold occurring between sheets in biotite and chlorite. (3) Subhedral to euhedral grains, up to 8  $\mu\text{m}$  across (Fig. 9C), are rare. Their shapes imply open-space deposition. (4) "Composite" grains, in which each grain of gold presents flat and cross-hatched aspects (Fig. 9D), only occur in the Maria Lázara samples,

where one part of the gold shows a close association with the Bi – Te – S multiphase grains. They are a few tens of micrometers in size.

The  $\text{HNO}_3$  attack has dissolved the bismuth, tellurium and sulfur, and the resulting textures reflect regularly alternating layers and intergrowths between the native gold and the Bi – Te – S minerals. In fact, they have similar crystallographic structures based on cubic close-packing (CCP) of atoms. In the absence of a replacement texture indicating Bi + Te addition to gold and because of the unique spatial distribution of this generation of gold (Ag < 5.5 at.%) with the Bi – Te – S minerals, this type of gold is considered to be contemporaneous with the Bi – Te – S minerals.

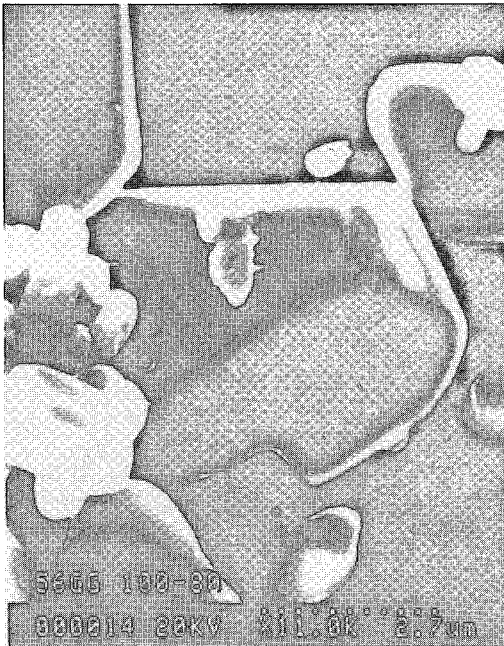
The cast-rich grains of group 2 may represent either (i) a secondary texture involving initially differently shaped grains of gold, which was acquired by



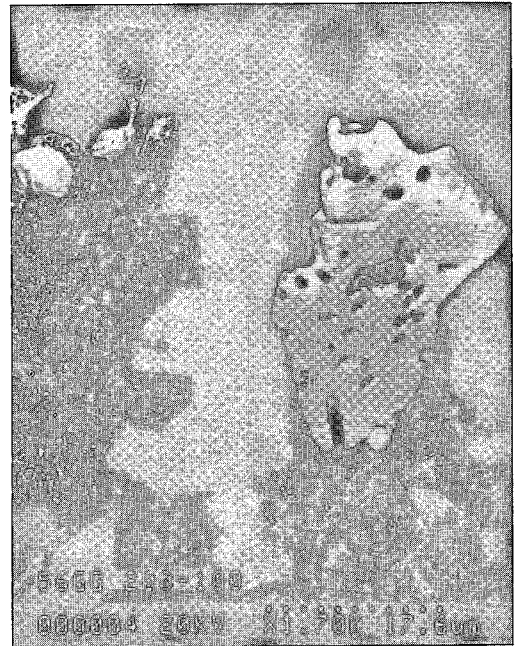
A



B



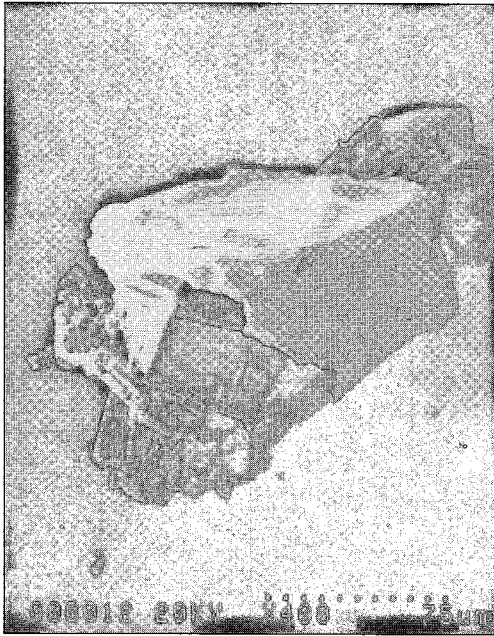
C



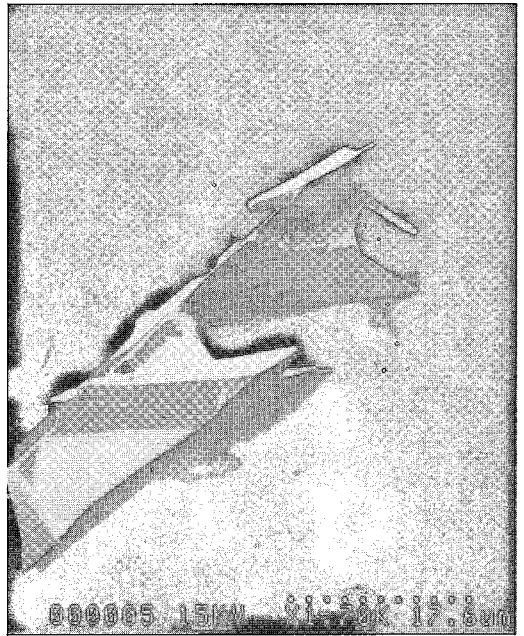
D

FIG. 9. The morphology of gold grains from María Lázara, as revealed by scanning electron microscopy. A. Thin plate of gold. B. Detail of a gold grain that shows successive straight growth-planes fitting the crystal faces of pre-existing sulfides. C. Euhedral grains of gold. D. "Composite" grain of gold revealed by the dissolution of Bi, Te and S during the  $\text{HNO}_3$  attack of a Au - Bi - Te - S multiphase grain.





A



B



C



D

FIG. 10. Morphology of gold grains from the Sigma mine, as revealed by scanning electron microscopy. A. Cast-rich grain on a residual grain of tourmaline (not dissolved by the hydrofluoric acid attack). B. Cast-rich grain with a shape typical of tourmaline cast. C. Detail of a gold grain showing successive straight growth-planes fitting the crystal faces of pre-existing tourmaline. D. Euhedral grain recovered from quartz.

“pressing” and molding the ductile grains against the nondeformable sulfides during episodes of vein deformation, or (ii) a primary texture in which the shapes of gold grains reflect the shapes of crystal faces of pre-existing sulfides. In case (i), each growth plane should have been distorted to mold the sulfides surfaces. Figure 9B proves that this is not the case, and that successive straight growth-planes fit the crystal faces of pre-existing sulfides. Therefore, cast-rich grains represent primary textures, and surface reactions with sulfides are likely involved in the deposition of gold.

### *Sigma*

The tourmaline grains were partially destroyed by the hydrofluoric acid attack. Two of the above-mentioned four morphological types were recovered: the cast-rich grains are very abundant, but they here show evidence of shapes typical of tourmaline castings (Figs. 10A, B). As in the case of the arsenopyrite casts previously noted, successive straight growth-planes fit the crystal faces of pre-existing tourmaline minerals (Fig. 10C). This suggests that cast-rich grains at Sigma are primary textures in which grain shapes reflect the shapes of crystal faces of pre-existing tourmaline. Some gold grains are thin and platy, without specific casts. Secondly, euhedral grains are very common, and show an octahedral habit (Fig. 10D). These grains correspond to the gold particles in healed microfractures.

## DISCUSSION OF THE RESULTS

The textural habits of gold grains may be compared to those observed in various geological settings and those recovered from experiments on mechanisms of gold deposition. Starling *et al.* (1989), Tarbayev (1991) and Knipe *et al.* (1992) have observed the development of gold grains with subspherical, domed shapes or euhedral shapes clustered close to pyrite or arsenopyrite surfaces in Precambrian gold-quartz veins. The grain size ranges from less than 1 to 750  $\mu\text{m}$ . In addition, globular-reniform grains of gold were found on sulfides from active vents on the seafloor (Herzig *et al.* 1990) and, also, on pyrite from the Carlin mine in Nevada (Bakken *et al.* 1989). Our data agree with these previous results in showing the importance of a sulfide substrate for deposition of gold.

Laboratory experiments have also demonstrated the importance of sulfide surfaces for gold deposition (Machairas 1970, Jean & Bancroft 1985, Hyland & Bancroft 1989, Renders & Seward 1989). In all experiments, gold appears with spherical shapes, and the grain size ranges from a few micrometers to 35  $\mu\text{m}$ . In the experiments of Machairas (1970) and Jean & Bancroft (1985), globular grains of gold formed very rapidly when auric chloride complexes entered in

contact with sulfide surfaces, as a result of  $\text{Au}^{3+}$  reduction on the surfaces of sulfide grains. After only one minute, globular grains were found to reach a diameter of several hundred nanometers, and to have shapes identical to the globular-reniform grains found in the Brazilian arsenopyrite-rich ores.

In the same experiments, grains of gold became visible to the naked eye after a few minutes and appeared as superimposed layers depending on the concentrations of Au in solution and the duration of reaction. Such grains look like the cast-rich grains from the Brazilian sulfide-rich ores and those associated with tourmaline at Sigma.

In conclusion, the observed globular-reniform and cast-rich grains of gold that precipitated onto earlier-formed S-rich arsenopyrite resemble those obtained by experimental reduction of gold on sulfide surfaces. It suggests that the reduction of gold on sulfides is a main process of deposition. The features of the casts related to tourmaline at Sigma also suggest the possibility of such surface reactions on tourmaline. This also applies to gold related to biotite at Maria Lázara. Both tourmaline and biotite are Fe-rich minerals.

The subhedral to euhedral grains of gold typically correspond to another process of gold deposition. Their habits imply the presence of open spaces during their growth, and their primary textural sites suggest a trapping contemporaneous with the precipitation of quartz. Such grains are abundant at Sigma, unlike the case of the Brazilian veins. The fact that the ores come from an extensional vein in the first case, and from shear veins in the second case, may explain the difference. Open-space filling textures are common in extensional veins at Sigma.

## PROCESS OF DEPOSITION OF GOLD

The development history of gold-quartz veins may correspond either to subsequent deformation occurring on already developed veins (Robert & Kelly 1987, Cathelineau *et al.* 1991) or to a complex sequence of stages of growth and deformation (Boullier & Robert 1992, Robert *et al.* 1995). Our data on the textural sites and the chemical compositions of gold grains rather support the latter hypothesis. Repeated deposition of gold occurs at every textural site as a result of repeated stages of vein deformation that produce fracturing or ductile deformation of pre-existing minerals. The habits of gold grains show the importance of sulfide and Fe-rich mineral surfaces on gold deposition. Gold reduction on earlier-formed minerals seems to be the main process of gold deposition in the three deposits studied.

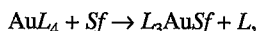
Recently, Möller & Kersten (1994) proposed an electrochemical cell model for deposition of gold. The authors experimented with an electrochemical cell obtained by the junction of *p*- and *n*-type sulfides. The *n*-type (negative) semiconductor is an electron donor,



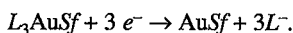
whereas the *p*-type (positive) is an electron acceptor. The *p/n* junction leads to electron transfer from *n*-type to *p*-type, and the latter then becomes the cell cathode. In H<sub>2</sub>S-saturated solutions, gold is accumulated at the cathode in cationic form (Au<sup>+</sup>).

In the present study, the main sulfide in the Brazilian samples is S-rich arsenopyrite (As/S < 1), which is an *n*-type semiconductor (Knipe *et al.* 1992, Möller & Kersten 1994) with a negative surface-charge. At Fazenda Brasileiro, pyrite without trace elements is also an *n*-type semiconductor, and the *p/n* junction does not exist (Möller & Kersten 1994). At Maria Lázara, As-rich arsenopyrite is a *p*-type semiconductor but never shows evidence of gold accumulation on its surfaces. The model of Möller & Kersten is therefore not applicable here.

Adsorption-reduction reactions on sulfide surfaces have been experimentally studied by Hyland & Bancroft (1989). The authors proposed a first step with the diffusion of ions in solution, with adsorption according to the following type of reaction:



where *L* represents the ligand, and *Sf*, the surface site. The second step is the reduction of cations:



In the case of such a mechanism, the main problem is the occurrence of identical charges between arsenopyrite and gold complexes in the fluids. Indeed, most of the gold in fluids of such deposits is interpreted to occur as negative gold thiosulfide complexes (Seward 1989, Shenberger & Barnes 1989). The diffusion and the adsorption of such gold complexes on the negatively charged arsenopyrite are impossible if complexes are not previously destroyed. Sibson *et al.* (1988) and Boullier & Robert (1992) have proposed that the fracturing of vein minerals is related to sudden failure and slip along shear veins or neighboring faults, accompanied by sudden drops of fluid pressure. Such inferred drops in fluid pressure may in turn induce destruction of the gold thiosulfide complexes, through boiling off of H<sub>2</sub>S. Then, the reduction of Au<sup>+</sup> to give Au<sup>0</sup> may occur easily on the *n*-type arsenopyrite (electron donors) once the auriferous fluid enters fractures and cavities. In the case of the Fe-rich minerals (tourmaline, biotite), the differences in normal oxidation potentials (E<sup>0</sup>) between Fe<sup>2+</sup>/Fe<sup>3+</sup> and Au<sup>0</sup>/Au<sup>+</sup> (respectively, -0.771 and -1.68 V) may allow the reduction of gold on surfaces of these minerals.

The remaining auriferous fluids may have been entrapped during deposition of quartz, with subsequent precipitation of subhedral to euhedral grains of gold. These shapes are abundant at Sigma because of the vein development in extensional fractures. This hypothesis implies that this gold is primary, related to a filling episode.

## CONCLUSIONS

An attempt has been made to clarify the causes and mechanisms of gold precipitation in quartz veins. The studies of gold grains based on their textural development, considering the Ag content and morphology, have revealed that:

1. Multistage deposition of gold occurs during repeated episodes of deformation, which supports the hypothesis that veins develop as a complex sequence of stages of growth and deformation (Boullier & Robert 1992).
2. The habit of gold grains shows the importance of surfaces of sulfide and Fe-rich minerals for deposition of gold. Reduction of gold on earlier-formed minerals seems to be a main process of gold deposition. Other gold grains show that gold also coprecipitates with the host quartz.

## ACKNOWLEDGEMENTS

The authors thank the CVRD (Cia Vale do Rio Doce) Brazilian company, Drs. A.M. Boullier and M.G. Pulz for their welcome and fruitful collaboration. Constructive comments by Dr. F. Robert and an anonymous reviewer are gratefully acknowledged. We express our thanks to Dr. K. Beets, who improved the English version.

## REFERENCES

- BAKKEN, B.M., HOHELLA, M.F., JR., MARSHALL, A.F. & TURNER, A.M. (1989): High-resolution microscopy of gold in unoxidized ore from the Carlin mine, Nevada. *Econ. Geol.* **84**, 171-179.
- BOULLIER, A.M. & ROBERT, F. (1992): Palaeoseismic events recorded in Archaean gold-quartz vein networks, Val d'Or, Abitibi, Quebec, Canada. *J. Struct. Geol.* **14**, 161-179.
- BOYLE, R.W. (1979): The geochemistry of gold and its deposits. *Geol. Surv. Can., Mem.* **280**.
- CATHELINÉAU, M., MARNIGNAC, C., BOIRON, M.C. & POTY, B. (1991): Hercynian gold-bearing quartz veins from western Europe. The "shear zone model" revisited. In *The Economics, Geology, Geochemistry and Genesis of Gold Deposits, Brazil Gold'91* (E.A. Ladeira, ed.). Balkema, Rotterdam, The Netherlands (115-119).
- HERZIG, P.M., FOUQUET, Y., HANNINGTON, M.D. & VON STACKELBERG, U. (1990): Visible gold in primary polymetallic sulfides from the Lau back-arc. *Trans. Am. Geophys. Union* **71**, 1680 (abstr.).
- HYLAND, M.M. & BANCROFT, G.M. (1989): An XPS study of gold deposition at low temperatures on sulphide minerals: reducing agents. *Geochim. Cosmochim. Acta* **53**, 367-372.

- JEAN, G.E. & BANCROFT, G.M. (1985): An XPS and SEM study of gold deposition at low temperatures on sulphide mineral surfaces: concentration of gold by adsorption/reduction. *Geochim. Cosmochim. Acta* **49**, 979-987.
- KNIFE, S.W., FOSTER, R.P. & STANLEY, C.J. (1992): Role of sulphide surfaces in sorption of precious metals from hydrothermal fluids. *Trans. Inst. Min. Metall.* **B101**, 83-88.
- MACHAIRAS, G. (1970): Contribution à l'étude minéralogique et métallographique de l'or. *Bull. B.R.G.M., deuxième sér.* **3**.
- MARIMON, M.P., KISHIDA, A. & TEIXEIRA, J.B. (1986): Estudo da alteração hidrotermal relacionada à mineralização aurífera na mina Fazenda Brasileiro (Bahia). XXXIV congresso Brasileiro de geol. (Goiânia), 1-14.
- MICHEL, D., GIULIANI, G., PULZ, G.M. & JOST, H. (1994): Multistage gold deposition in the Archaean Maria Lázara gold deposit (Goiás, Brazil). *Mineral. Deposita* **29**, 94-97.
- MÖLLER, P. & KERSTEN, G. (1994): Electrochemical accumulation of visible gold on pyrite and arsenopyrite surfaces. *Mineral. Deposita* **29**, 404-413.
- NEUERBURG, G.J. (1975): A procedure, using hydrofluoric acid, for quantitative mineral separations from silicate rocks. *J. Res. U.S. Geol. Surv.* **3**, 377-378.
- PHILLIPS, G.N. & GROVES, D.I. (1984): Fluid access and fluid - wall rock interaction in the genesis of the Archaean gold-quartz vein deposit at Hunt mine, Kambalda, Western Australia. In *The Geology, Geochemistry and Genesis of Gold Deposits, Gold'82* (R.P. Foster, ed.). A.A. Balkema, Rotterdam, The Netherlands (389-416).
- PULZ, M.G. (1990): *Geologia do depósito aurífero tipo Maria Lázara (Guarinos-Goiás)*. Dissertação de Mestrado, Univ. de Brasília, Brasília, Brazil.
- \_\_\_\_\_, JOST, H., GIULIANI, G. & MICHEL, D. (1991): Maria Lázara gold deposit (Goiás State, Brazil): an example of intense fluid/rock interaction associated with a triple point structure. In *Source, Transport and Deposition of Metals* (M. Pagel & J.L. Leroy, eds.). A.A. Balkema, Rotterdam, The Netherlands (117-118, abstr.).
- REINHARDT, M.C. & DAVISON, I. (1990): Structural and lithologic controls on gold deposition in the shear zone-hosted Fazenda Brasileiro mine, Bahia state, northeast Brazil. *Econ. Geol.* **85**, 952-967.
- RENDERS, P.J. & SEWARD, T.M. (1989): The adsorption of thio gold(I) complexes by amorphous  $As_2S_3$  and  $Sb_2S_3$  at 25 and 90°C. *Geochim. Cosmochim. Acta* **53**, 255-267.
- ROBERT, F. & BOULLIER, A.-M. & FIRDAOUS, K. (1995): Gold-quartz veins in metamorphic terranes and their bearing on the role of fluids in faulting. *J. Geophys. Res.* **100**, 12,861-12,879.
- \_\_\_\_\_, & BROWN, A.C. (1986): Archean gold-bearing quartz veins at the Sigma mine, Abitibi greenstone belt, Quebec. II. Vein paragenesis and hydrothermal alteration. *Econ. Geol.* **81**, 593-616.
- \_\_\_\_\_, & KELLY, W.C. (1987): Ore-forming fluids in Archean gold-bearing quartz veins at the Sigma mine, Abitibi Greenstone Belt, Quebec, Canada. *Econ. Geol.* **82**, 1464-1482.
- SEWARD, T.M. (1989): The hydrothermal chemistry of gold and its implications for ore formation: boiling and conductive cooling as examples. *Econ. Geol., Monogr.* **6**, 398-404.
- SHENBERGER, D.M. & BARNES, H.L. (1989): Solubility of gold in aqueous sulfide solutions from 150 to 350°C. *Geochim. Cosmochim. Acta* **53**, 269-278.
- SIBSON, R.H., ROBERT, F. & POULSEN, K.H. (1988): High-angle reverse faults, fluid-pressure cycling and mesothermal gold-quartz deposits. *Geology* **16**, 551-555.
- STARLING, A., GILLIGAN, J.M., CARTER, A.H.C., FOSTER, R.P. & SAUNDERS, R.A. (1989): High-temperature hydrothermal precipitation of precious metals on the surface of pyrite. *Nature* **340**, 298-300.
- TARBAYEV, M.B. (1991): Typomorphism of gold crystals from quartz reefs. In *The Economics, Geology, Geochemistry and Genesis of Gold Deposits, Brazil Gold'91*. (E.A. Ladeira, ed.). A.A. Balkema, Rotterdam, The Netherlands (353-357).
- TEIXEIRA, J.B.G., KISHIDA, A., MARIMON, M.P.C., XAVIER, R.P. & MCREATH, I. (1990): The Fazenda Brasileiro gold deposit, Bahia: geology, hydrothermal alteration and fluid inclusion studies. *Econ. Geol.* **85**, 990-1009.

Received May 25, 1994, revised manuscript accepted January 3, 1996.